Embryonic Nuclei-Induced Alloying Process for the Reproducible Synthesis of Blue-Emitting $Zn_xCd_{1-x}Se$ Nanocrystals with Long-Time Thermal Stability in Size Distribution and Emission Wavelength

Xinhua Zhong,*,†,‡ Zhihua Zhang,† Shuhua Liu,† Mingyong Han,†,‡ and Wolfgang Knoll*,†

Department of Materials Science, National University of Singapore and Institute of Materials Research & Engineering, Singapore 117543

Received: May 5, 2004; In Final Form: July 10, 2004

High-quality short-wavelength-emitting $Zn_xCd_{1-x}Se$ nanocrystals with emission wavelengths tunable from 440 to 550 nm have been prepared through the incorporation of a Zn precursor into the newly formed CdSe nuclei together with the remaining Cd/Se precursors (or Cd precursor into the ZnSe nuclei with the remaining Zn/Se precursors). The photoluminescence properties for the obtained alloyed nanocrystals (emission efficiencies of 45−70%, fwhm = 24−32 nm) are comparable to or even better than those for the best-reported binary nanocrystals. Moreover, the alloyed nanocrystals can retain their high luminescence (emission efficiency of ∼30%) if dispersed in aqueous solution. The most striking feature of the alloyed nanocrystals is their unusual long-time stability in emission wavelength/color, spectral width, and emission efficiency at high temperature. This is attributed to their characteristic structure (increased covalency and hardened lattice) and the strong bonding capability of the coordinating surfactant trioctylphosphine oxide to dangling Zn bonds at the surface of the alloyed nanocrystals. Through the embryonic nuclei-induced alloying process, highly luminescent and stable nanocrystals with different desired emission wavelengths/colors can be achieved reproducibly by only changing the synthetic recipe through adding the predetermined amount of reaction precursors. It is expected that the reported effective synthetic strategy can be developed into a very practical approach to high-quality color-tunable nanocrystals with narrow spectral width and high stability.

Introduction

Colloidal semiconductor nanocrystals (quantum dots, QDs) have attracted great attention for their distinguished role in fundamental studies and technical applications[1] such as light-emitting devices,[2−5] lasers,[6,7] and biological labels.[8−12] Owing to their unique size-dependent photoluminescence (PL) tunable across the visible spectrum, the binary cadmium chalcogenides, in particular CdSe, have been the most extensively studied system among the various semiconductor nanomaterials. In the last two decades, the main efforts have been focused on the preparation of size-tunable binary or core−shell nanocrystals with different emission colors.[13−19] However, the tuning of physical and chemical properties by changing the particle size could cause problems in many applications, in particular, if unstable/reactive small particles (less than ∼2 nm) are used. Consequently, with the current protocols and modification of high-temperature organometallic methods, the best-reported PL efficiency of over 50% is limited to the emission wavelength above 520 nm for relatively large CdSe nanocrystals.[13−19] This is because very small CdSe nanocrystals with a band-edge emission in the blue spectral region remain very difficult to passivate and exhibit low emission efficiency and a broad spectral width. Theoretically, wider band-gap materials such as CdS and ZnSe can also be used to prepare blue-emitting nanocrystals; however, their photoluminescence properties are not very stable in practice. Since the size-tunable emission strategy can only lead to the preparation of green- and red-emitting nanocrystals so far, it still remains a challenge for materials scientists to develop new synthetic methods to make highly luminescent and stable nanocrystals, especially blue-emitting ones.

Recent advances have led to the exploration of composition-tunable emission by changing their constituent stoichiometries in ternary composite nanocrystals.[20−25] Recently, we reported alloyed $Zn_xCd_{1-x}E$ (E = Se, or S) nanocrystals with color-tunable emission via the variation of the particle composition besides the particle size.[26,27] The luminescence properties of the reported alloyed nanocrystals are comparable to or even better than the best-reported binary CdSe-based nanocrystals. In the previous study,[26] $Zn_xCd_{1-x}Se$-alloyed nanocrystals were prepared via the incorporation of Zn/Se into the preprepared highly luminescent stable CdSe nanocrystals (∼5 nm in diameter) at high temperature. As the obtained CdSe nanocrystals have a relatively large size, this method is limited to synthesizing nanocrystals with an emission wavelength above 490 nm. To obtain shorter wavelength-emitting $Zn_xCd_{1-x}Se$ nanocrystals, very small CdSe particles as initial seeds are required. Practically it is not easy to obtain very small, stable CdSe nanocrystals because CdSe nuclei seeds can grow very quickly during the reheating process for the preparation of the alloyed nanocrystals.

In this paper we report an embryonic nuclei-induced alloying process for the preparation of highly luminescent stable blue-emitting $Zn_xCd_{1-x}Se$ nanocrystals. A two-step synthetic procedure was designed to separate the nucleation process from the crystal growth for alloyed nanocrystals. It is known that consecutive nucleation and growth stages are involved in the

* To whom correspondence should be addressed: E-mail: zhong_xinhua@alumni.nus.edu.sg.
† National University of Singapore.
‡ Institute of Materials Research and Engineering.

10.1021/jp048071y CCC: $27.50
Published on Web 09/10/2004

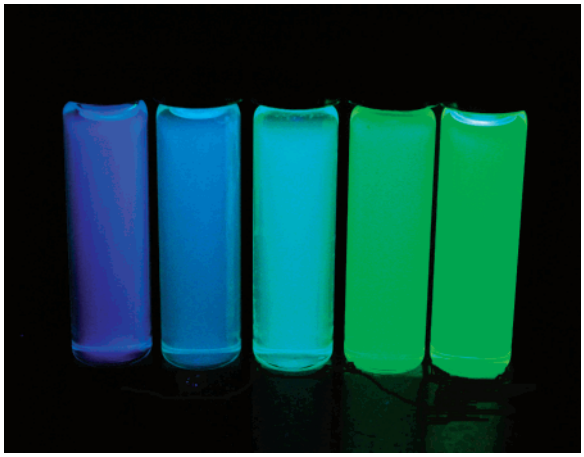

Figure 1. Composition-tunable emission colors of the obtained $Zn_xCd_{1-x}Se$ nanocrystals in the blue-to-green spectral region excited with a UV lamp.

formation of colloidal nanocrystals.[28] If the nuclei are larger than the critical size, a stable diffusion-driven growth process proceeds spontaneously.[29] In our experiment, after the CdSe nuclei reached beyond the critical size (referred to as embryonic nuclei hereinafter), Zn precursor was loaded into the reaction mixture immediately. The embryonic CdSe nuclei further served as seeds for the subsequent crystal growth where the injected Zn precursors and the existing Cd/Se monomers were incorporated into the embryonic nuclei together for the formation of larger $Zn_xCd_{1-x}Se$ nanocrystals. Analogously, $Zn_xCd_{1-x}Se$-alloyed nanocrystals can also be made via the incorporation of Cd precursor into the preformed embryonic ZnSe nuclei seeds together with the existing Zn/Se monomers.

The reported embryonic nuclei-induced alloying approach provides an effective way to produce highly luminescent short wavelength-emitting $Zn_xCd_{1-x}Se$ nanocrystals with narrow spectral width and high stability (Figure 1). As the obtained high-quality nanocrystals with unusual long-term stability in emission wavelength and spectral width at high temperature, the composition-tunable nanocrystals with desired emission wavelengths or colors can be achieved reproducibly by only changing the synthetic recipe through adding the predetermined amount of reaction precursors. The obtained highly thermally stable blue-emitting nanocrystals should be ideal materials for short-wavelength optoelectronic devices and can potentially provide a stable primary blue color for display applications. The high-quality blue-emitting nanocrystals can also act as a new color for biological labels for sensitive, multicolor, and multiplexing applications. The embryonic nuclei-induced alloying process has been proven to be a highly reproducible approach to high-quality color-tunable nanocrystals, and this synthetic strategy is being developed into a practical method for commercial applications.

Experimental Section

Chemicals. Trioctylphosphine oxide (TOPO, 90%), trioctylphosphine (TOP, 90%), hexadecylamine (HDA, 90%), stearic acid (95%), and Se powder (99.999%) were purchased from Aldrich. CdO (99.999%), diethylzinc (95%), and dimethylcadmium (95%) were purchased from Strem.

Synthesis of $Zn_xCd_{1-x}Se$ Nanocrystals Starting from CdSe Seeds. Typically, 0.0128 g (0.1 mmol) of CdO and 0.11 g (0.4 mmol) of stearic acid were loaded into a 25-mL three-neck round-bottom flask and the mixture was heated to 180 °C under an argon atmosphere until a clear solution was formed. After the reaction solution was cooled to room temperature, 2.0 g of TOPO and 2.0 g of HDA were added to the flask. The mixture was dried and degassed in the reaction vessel by heating to 100 °C at 0.1 Torr for 1 h while flushing the reaction system periodically with a flow of argon at least three times. After the reaction temperature was further increased and stabilized at 320 °C with stirring under a flow of argon, a 1.0-mL solution of Se (0.039 g, 0.5 mmol) in TOP was swiftly injected into the reaction flask. To this reaction mixture was then added a 1.0-mL solution of $ZnEt_2$ (0.2 mmol) in TOP immediately after the reaction solution turned from colorless to light red (~5 s after the addition of Se solution). The temperature was further set at 310 °C for the subsequent growth and annealing process of nanocrystals (After the addition of Se and Zn solutions, the temperature dropped to ~300 °C instantly and returned to 310 °C within ~2−3 min). Aliquots of the sample were taken at different time intervals and injected into cold chloroform (25 °C) to terminate the growth of nanocrystals quickly so they could be used to record their UV−vis and PL spectra. When $Zn_xCd_{1-x}Se$ nanocrystals reached the desired emission wavelength, the heater was removed and the reaction mixture was cooled to room temperature. Under identical conditions, different amounts of Zn precursor were used for the preparation of different color-emitting $Zn_xCd_{1-x}Se$ nanocrystals with different compositions.

Synthesis of $Zn_xCd_{1-x}Se$ Nanocrystals Starting from ZnSe Seeds. An operation procedure similar to the above one was used. Typically, 2.0 g of TOPO and 2.0 g of HDA were first loaded into a flask. After being thoroughly degassed under vacuum at 100 °C, the mixture was heated to 320 °C. To the reaction vessel was then added a 1.0-mL solution of Se (0.039 mg, 0.5 mmol) in TOP. Once the temperature was stabilized at 320 °C, a 1.0-mL solution of $ZnEt_2$ (0.20 mmol) in TOP was swiftly injected into the reaction system, 5 s later followed by a 1.0-mL solution of $CdMe_2$ (0.15 mmol) in TOP. The reaction mixture was then kept at 310 °C for the subsequent growth and annealing process of nanocrystals. Under identical conditions, different amounts of Cd precursor were used for the preparation of different color-emitting $Zn_xCd_{1-x}Se$ nanocrystals with different compositions.

Characterization. The obtained QDs in chloroform solution were precipitated with methanol and further isolated by centrifugation and decantation. The excessive ligands and reaction precursors were removed by extensive purification prior to the measurements using high-resolution transmission electron microscopy (HR-TEM), powder X-ray diffraction (p-XRD), inductively coupled plasma atomic emission (ICP), and X-ray photoelectron spectroscopy (XPS). All of the measurements were performed on original QD samples without any size sorting. A JEOL JEM3010 transmission electron microscope (operated at an accelerating voltage of 300 kV) was used to analyze size, size distribution, and structure of the final products deposited on the Formvar-carbon-coated copper grids. The XRD patterns for the alloyed nanocrystals were recorded by a Siemens D5005 X-ray powder diffractometer. The compositions for the alloyed nanocrystals were measured by means of ICP using a standard HCl/HNO_3 digestion. The XPS experiments were performed on a VG ESCALAB 220i-XL instrument with an Al Kα X-ray source. The binding energy was calibrated with the C1s line (284.8 eV). The obtained XPS spectra were analyzed using a peak synthesis program whereby a Shirley background was chosen and the fitting peaks of the experimental data were defined by a combination of 50% Gaussian and 50% Lorentzian after the optimization. UV−Vis and PL spectra were

obtained on a Shimadzu UV-1601 spectrometer and a RF-5301 PC fluorometer, respectively. The room-temperature PL efficiencies were determined by comparing the integrated emission of the QDs samples to that of dyes in solutions. The absorption spectra of both the dye and the nanocrystal sample were measured and the wavelength corresponding to the point of intersection of the both absorption spectra was used as the excitation wavelength for recording their emission spectra. The dyes (such as rhodamine 6G or coumarin 540) should have significantly overlaps in PL spectra with the QDs to be measured. A quadratic refractive index correction was done when two different solvents were used to dissolve QDs and dyes.[30] Also, the known efficiencies of the QDs in chloroform can be used to measure the efficiencies of other QDs by comparing their integrated emission or PL intensity of solutions. Low concentration of solution was used to avoid obvious reabsorption.

Results and Discussion

Nuclei-Induced Growth of $Zn_xCd_{1-x}Se$ Nanocrystals. The as-synthesized nanocrystals were routinely investigated by TEM and p-XRD to collect statistically reliable data for the dependence of nanocrystal size, shape, and crystallinity on various reaction parameters. The obtained nanocrystals have a nearly spherical shape with a narrow size distribution (relative standard deviation of 5−11%) and high crystallinity confirmed by TEM and HR-TEM (Figure 2). With the increase of reaction time, the resulting nanocrystals grew gradually. The particle size increased from 3.1 to 4.3 nm upon the extension of the heating time from 30 to 180 min (Figure 2). The corresponding Zn molar fraction increased from 0.46 to 0.61 in the obtained $Zn_xCd_{1-x}Se$ particles starting from CdSe seeds (confirmed by ICP and p-XRD). The high crystallinity of these wurtzite nanocrystals was also confirmed by p-XRD. The diffraction patterns of the wurtzite $Zn_xCd_{1-x}Se$ nanocrystals are located between those for wurtzite CdSe and ZnSe materials. The dependence of the diffraction peak positions of the obtained alloyed nanocrystals on their corresponding compositions is in accordance with Vegard's law, which provides an alloying evidence.[31]

The strong size or composition dependence of optical properties of semiconductor nanocrystals was monitored to reflect mean particle size and size distribution through the temporal evolution of UV−visible and PL spectra. Figure 3 shows the absorption and PL spectra of $Zn_xCd_{1-x}Se$ samples taken from the reaction flasks at different reaction times or stages for crystal growth. For each $Zn_xCd_{1-x}Se$ sample, the small Stokes shift between the emission and excitonic absorption peaks indicates the dominant band-edge luminescence in the $Zn_xCd_{1-x}Se$ nanocrystals. In the case of $Zn_xCd_{1-x}Se$ samples prepared from CdSe seeds, both their absorption and PL spectra shifted to shorter wavelengths in the first 120 min as a consequence of the increased Zn molar ratio. Only after prolonged excessive heating for a long period of time did the absorbance and emission peaks red shift to longer wavelengths due to Oswald ripening (Figure 3A). However, in the case of $Zn_xCd_{1-x}Se$ samples starting from ZnSe seeds, both their absorption and the PL spectra red-shifted to longer wavelengths at the early growth stage, and the peaks red-shifted further after a long period of a stable stage (Figure 3B).

Long-Term Thermal Stability of $Zn_xCd_{1-x}Se$ Nanocrystals in Emission Wavelength and Size Distribution. In the preparation of binary semiconductor nanocrystals, usually with the depletion of reaction precursors (or monomers), Ostwald ripening (defocusing of size distribution) occurs subsequently, where larger particles grow at the expense of small ones because small particles have higher solubility than larger ones.[13−15]

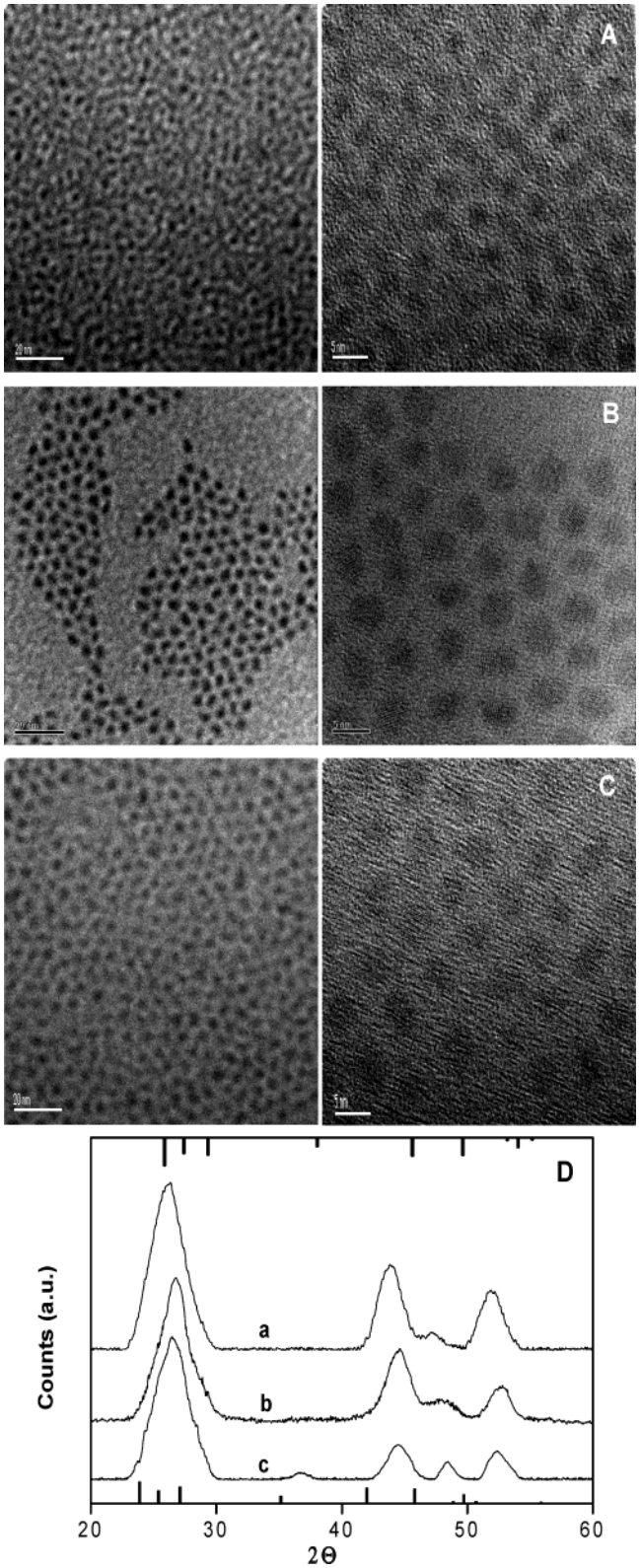

Figure 2. Wide-field TEM and HR-TEM micrographs of (A) 3.1-nm $Zn_{0.46}Cd_{0.54}Se$ and (B) 4.3-nm $Zn_{0.61}Cd_{0.39}Se$ nanocrystals starting from CdSe seeds corresponding to the growth periods of 30 and 180 min, respectively. (C) 4.1-nm $Zn_{0.64}Cd_{0.36}Se$ starting from ZnSe seeds corresponds to the growth period of 180 min. (D) The corresponding p-XRD patterns of the $Zn_xCd_{1-x}Se$ nanocrystals. The line spectra indicate the reflections of hexagonal bulk CdSe (bottom) and ZnSe (top) materials.

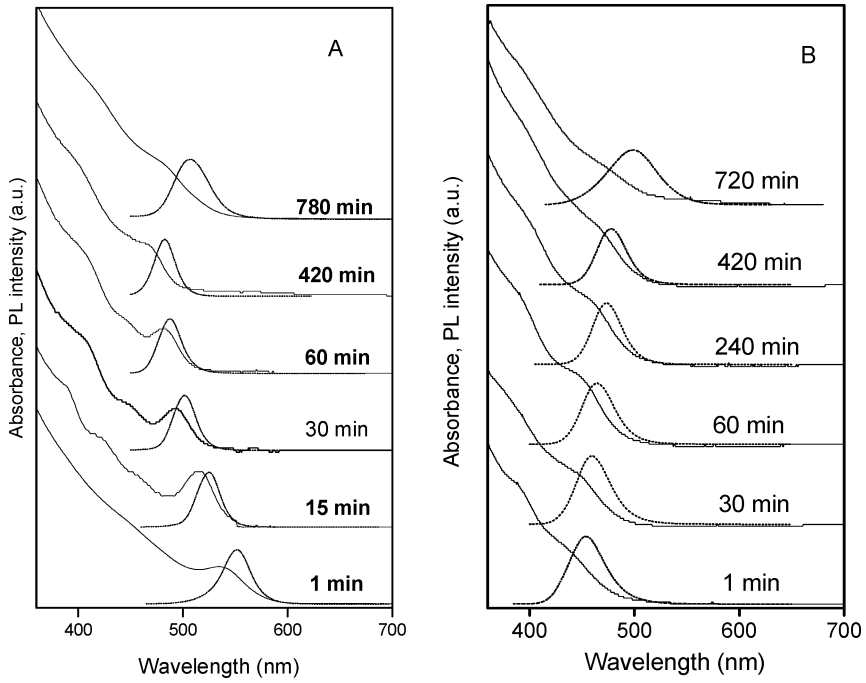

Figure 3. UV−Vis absorption and PL spectra (λ_{ex}=340 nm, right) of $Zn_xCd_{1-x}Se$ nanocrystals at different growth time starting from (A) CdSe seeds and (B) ZnSe seeds, respectively.

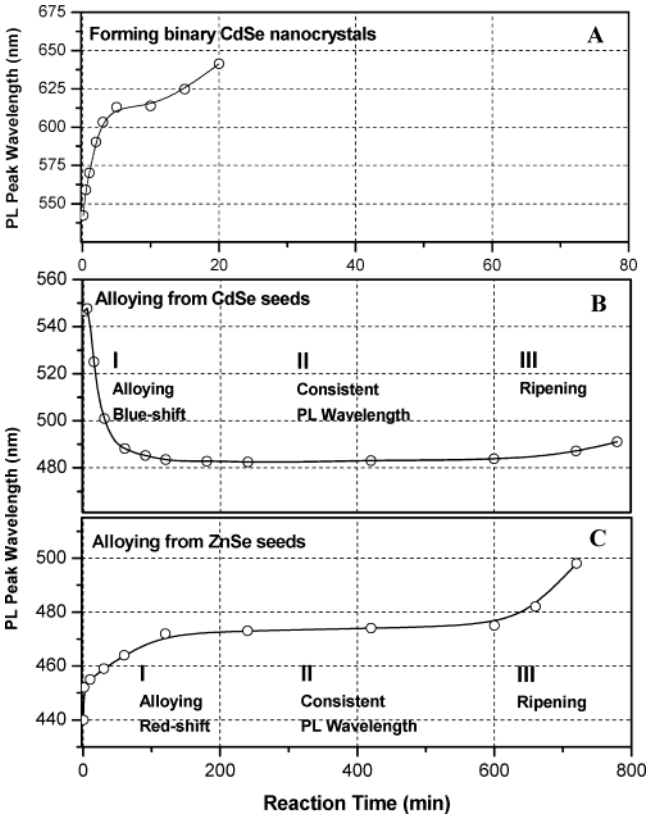

Figure 4. Temporal evolution of the PL peak wavelengths of (A) the binary CdSe nanocrystals, the ternary $Zn_xCd_{1-x}Se$-alloyed nanocrystals starting from CdSe seeds (B) and ZnSe seeds (C) during the growth process of nanocrystals at 310 °C under identical coordinating solvent system.

Figure 4A shows the typical growth kinetics of plain binary CdSe nanocrystals synthesized at identical conditions for the ternary $Zn_xCd_{1-x}Se$ nanocrystals. In the initial stage, an immediate red shift in emission wavelength was observed due to the instant nucleation and growth process. However, after a short period in which there was a stable stage (∼5−10 min), the PL peak red-shifted further due to a ripening effect. Their fluorescence was quenched gradually in the course of ∼30 min.

Very different growth kinetics of the alloyed nanocrystals were observed as compared to those of the binary CdSe nanocrystals. In the preparation of $Zn_xCd_{1-x}Se$ nanocrystals starting from CdSe seeds (Figure 4B), during the first 120 min after the addition of $ZnEt_2$, a significant sharp blue shift in the emission wavelength occurred accompanied by an increase of average particle size (confirmed by TEM results). With the extension of heating time up to 180 min, the emission peak systematically blue-shifted from 547 to 482 nm. This blue shift results from the progressive incorporation of the wider band-gap ZnSe (E_g = 2.62 eV) into the initial narrower band-gap CdSe seeds (E_g = 1.74 eV) along with the cogrowth of the existing Cd/Se precursors to form alloyed $Zn_xCd_{1-x}Se$ nanocrystals. After this alloying process, the subsequent heating (∼7 h) did not cause a shift of the emission peak, which indicates that there is no detectable change in particle size and the well-formed nanoparticles have reached or grown up to a stable size. The prolonged excessive heating over 10 h led to an obvious red shift in emission wavelength occurring via a ripening process. In the case of $Zn_xCd_{1-x}Se$-alloyed nanocrystals starting from ZnSe seeds (Figure 4C), as the narrower band-gap CdSe was incorporated into the wider band-gap ZnSe seeds, a clear red shift in wavelength took place during the alloying stage due to the coherent effect of the increase of particle size and the decrease of band-gap energy in the obtained $Zn_xCd_{1-x}Se$ nanocrystals. After excessive heating to 10 h, an Ostwald ripening process of the alloyed nanocrystals occurred very slowly, leading to a red shift in the emission wavelength and a broadening in the spectral width. This may result from the progressive decomposition or oxidation of the organic capping reagents and these ligands may desorb from the particle surface. As the capping effect was weakened with the changes of interfacial properties, the ripening occurred accordingly. It should be noted that the higher ratio of HAD to TOPO would

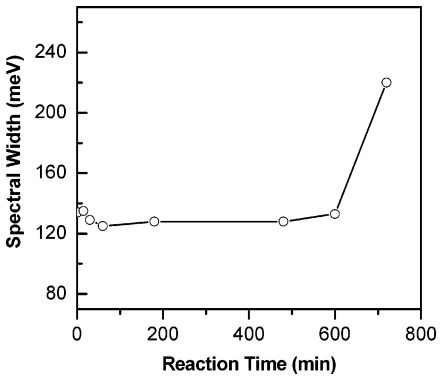

Figure 5. Temporal evolution of PL spectral width of the obtained $Zn_xCd_{1-x}Se$ nanocrystals starting from CdSe seeds.

favor the formation of alloyed nanocrystals in the synthetic system. However, the mass ratio of HDA/TOPO cannot be larger than 4. Otherwise, the photoluminescence intensity of the resulting alloy nanocrystals will be gradually quenched after 3 h of heating.

As the PL spectral width can reflect the size distribution of nanocrystals, the temporal evolution of the spectral width of the $Zn_xCd_{1-x}Se$ nanocrystals starting from CdSe seeds was monitored as well. Three evolution stages are demonstrated clearly in Figure 5 during the progressive incorporation of Zn monomers into CdSe seeds. With the proceeding of the alloying progress, (i) the PL spectral width gradually decreased to the minimum value of 125 meV from 135 meV in the first 60 min with the depletion of precursors and the completion of crystal growth, (ii) the minimum spectral width was then kept for a long period, and (iii) finally the spectral width increased with continuous heating after 10 h. The narrowing in spectral width at the alloying stage can be explained by a "focusing" mechanism for the growth of semiconductor nanocrystals because smaller particles have a faster growth rate than larger ones in an ensemble.[32,33] In the case for the formation of $Zn_xCd_{1-x}Se$ nanocrystals starting from ZnSe seeds, no obvious size-focusing effect was observed (the spectral width remained unchanged during the annealing process until ripening occurred.).

One of the most interesting features in the growth kinetics of alloyed nanocrystals is the unusual long-term fixation of the PL peak position and fluoresce efficiency. This indicates that the obtained alloyed nanocrystals can maintain a consistent PL wavelength and spectral width (constant composition and identical particle size/size distribution) during the 7 h heat treatment. This may be due to the characteristic properties of the alloy nanocrystals and the existence of the strong capping ligands as discussed below. The absence of Ostwald ripening in the growth process demonstrates that the transformation of molecular precursors to nanocrystals is either irreversible or an equilibrium process between monomers and nanocrystals. This inherent mechanism may result from an increased covalency and reduced ionicity of the $Zn_xCd_{1-x}Se$-alloyed nanocrystals because the stronger Zn−Se bond can stabilize the weaker Cd−Se bond. This leads to a hardened lattice structure and a lower solubility of $Zn_xCd_{1-x}Se$ nanocrystals as compared to the plain CdSe. Also, this unique property may be caused by the strong bonding capability of TOPO to Zn at the surface of the alloyed nanocrystals. This assumption is in agreement with previous experimental results that the strong ligand TOPO can stabilize Zn precursor via forming Zn−TOPO complexes at high temperature.[34] Very supportive evidence comes from the finding that ZnSe nanocrystals cannot be formed in the TOPO/TOP coordinating solvent system.[34] The stable Zn−TOPO complexes can explain the reason why the alloying process proceeds slowly (∼2 h) because a high monomer concentration can be maintained for the continuous slow growth of the alloyed nanocrystals. The observed absence of the Ostwald ripening process is commonly observed in the growth process of colloidal metal nanocrystal systems,[35−37] but it is very scarce in the colloidal semiconductor nanocrystal systems because most metal nanocrystals usually cannot dissolve in the reaction solvent system. On the contrary, most semiconductor nanocrystals can do this.

Reproducible Synthesis of Color-Tunable $Zn_xCd_{1-x}Se$ Nanocrystals with Predetermined Emission Wavelength via Changing Synthetic Recipes. The emission wavelength of the alloyed $Zn_xCd_{1-x}Se$ nanocrystals during the stable region is mainly dependent on the amounts of Zn and Cd precursors used. In the preparation of $Zn_xCd_{1-x}Se$ nanocrystals starting from CdSe seeds, under a fixed amount of Cd-precursor, the emission wavelength of the final resulting alloyed nanocrystals blue-shifted systematically with the increase of the amount of Zn precursor used because a higher Zn molar fraction can be reached in the final alloyed nanocrystals. Under conditions stated in the experiment, the emission wavelength of the obtained alloyed nanocrystals changed from ∼550 to 460 nm after 2 h of heat treatment when the amount of $ZnEt_2$ was increased from 0.1 to 0.4 mmol (Figure 6a). Similarly, in the preparation of $Zn_xCd_{1-x}Se$ nanocrystals starting from ZnSe seeds, the relative higher amount of Cd precursors to Zn seeds can result in a longer emission wavelength of the alloyed $Zn_xCd_{1-x}Se$ nanocrystals (Figure 6b). That is to say, different emission wavelengths of the alloyed nanocrystals can be achieved by simply changing the synthetic recipe with different predetermined amounts of precursors. It is surprising that the emission wavelength of the finally obtained alloyed nanocrystals in the stable region is independent of the addition rate of Zn (or Cd) precursor. In addition, there was no obvious difference in the

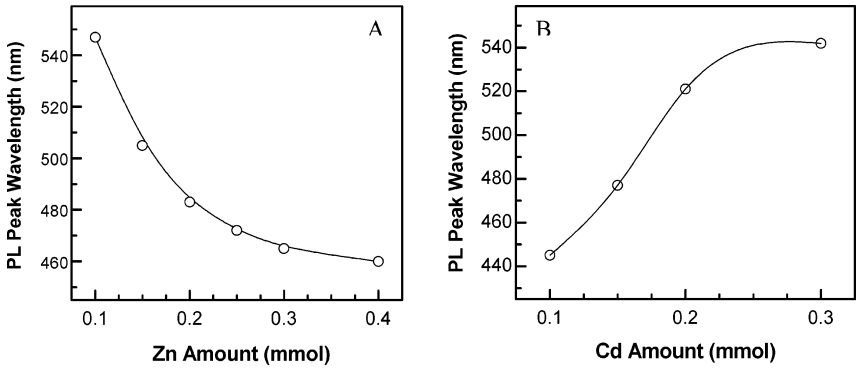

Figure 6. Dependence of PL peak wavelength on the amount of (A) Zn precursor or (B) Cd precursor added into the reaction system containing CdSe or ZnSe nuclei seeds, respectively.

emission wavelength of the obtained alloyed nanocrystals if the Zn (or Cd) precursor was introduced at different reaction times (from 3 to 10 s) after the nucleation process. The variation of growth temperature mainly affects the alloying rate and has no significant effect on the final emission wavelength of the alloyed nanocrystals. However, if the temperature is too low (<270 °C), no alloying process was observed. These features make this synthetic approach very reproducible for the preparation of highly luminescent and stable $Zn_xCd_{1-x}Se$ nanocrystals.

Optical Properties. The alloyed $Zn_xCd_{1-x}Se$ nanocrystals prepared by this synthetic approach have very good PL properties, such as the ones reported previously.[26] For the nanocrystal samples grown within the first 8 h of annealing, the PL emission efficiencies are ~45−70% at room temperature and the spectral widths are ~24−32 nm. With the proceeding of the alloying process, the emission efficiencies for the instant samples increased steadily until they reached the highest value at the stable stage. The feature that the highest quantum yield can be maintained for several hours makes this synthetic strategy a very practical approach to highly luminescent nanocrystals. In the following ripening stage, the emission efficiencies decreased gradually. In comparison, the PL emission efficiency of plain binary CdSe nanocrystals decreased to zero after an annealing process of ~30 min at the same conditions. If hydrophilic reagents such as mercaptoacetic acid replaced the organic capping reagents of the obtained $Zn_xCd_{1-x}Se$ nanocrystals,[9] the resulting water-soluble nanocrystals could still retain a high photoluminescence efficiency of ~25−35%. The high emission efficiency of the obtained alloyed nanocrystals may profit from the specified growth conditions (high preparation temperature, excess of Se monomer, optimum composition of coordination solvents, etc.). The long-term annealing at high temperatures may promote surface ordering and reconstruction, resulting in a reduction of the defect concentration formed at the early stage of nanocrystal formation and an increase of their emission efficiencies and crystallinity accordingly.[38] The existence of the strong bonding reagent TOPO leads to a large monomer oversaturation, resulting in slow growth, high emission efficiency, and narrow size distribution of nanocrystals.[15a,33,39] As reported by Weller,[33] the nanoparticles with the lowest rate of growth within an ensemble were assumed to have the lowest degree of surface disorder and therefore the highest PL emission efficiency. An excess of Se precursor is also essential to achieve high emission efficiency, which has been investigated by Peng and Donega, respectively.[15a,37]

Alloying Analysis. The most direct evidence for alloying process can be probed from the absorption and PL spectra of the obtained $Zn_xCd_{1-x}Se$ nanocrystals. The sole absorption and PL peak in their spectra can rule out the separate nucleation of ZnSe and CdSe, which is in agreement with the results from TEM and XRD measurements. With the increase of the Zn molar fraction in the resulting nanocrystals, a systematic blue shift was observed for both the first excitonic absorption onsets and the band-edge emission peaks (Figures 3 and 4). This systematic blue shift upon the increase in Zn content provides clear evidence for the formation of alloyed $Zn_xCd_{1-x}Se$ nanocrystals rather than separate ZnSe and CdSe particles, or core−shell-structured nanocrystals.[25−27,40] If a core−shell structure is formed, such a significant shift of optical spectra cannot be produced as compared with those of the "core" materials.[16−18] In addition, the observed narrow and symmetric PL peak supports the formation of a homogeneous alloy structure (solid solution) rather than a structure with random spatial compositional fluctuations. Furthermore, the dependence of the XRD peak positions of the obtained $Zn_xCd_{1-x}Se$ particles (the experimental lattice parameter c) on their corresponding composition is in accordance with Vegard's law, indicating the formation of the alloyed $Zn_xCd_{1-x}Se$ nanocrystals with a homogeneous distribution of ZnSe and CdSe.[31]

TABLE 1: Zn:Cd Molar Ratios Measured by ICP or XPS for Alloyed and Core−Shell Nanocrystals

nanocrystal samples	ICP results	XPS results
alloyed $Zn_xCd_{1-x}Se$ from ZnSe seeds	1.78:1	1.92:1
alloyed $Zn_xCd_{1-x}Se$ from CdSe seeds	1.56:1	1.58:1
core-shell CdSe/ZnSe	1.07:1	5.55:1

XPS results provide further evidence for an alloy rather than a core−shell structure of the resulting nanocrystals. In the XPS spectrum, the intensity of the photoelectron signal originating from a given atom is defined by $I = I_0e^{(-z/\lambda)}$ where I_0 is the unattenuated signal intensity, z is the distance of the emitting atom from the surface, and λ is the mean free path (or escape depth) of the emitted electron. Due to the increased z, the probability for detecting a photoelectron from an atom buried in the material is significantly smaller than that from an atom near the surface. The relative concentrations of Zn and Cd are calculated by dividing the area of XPS signals by their respective sensitivity factors. For comparison, core−shell ZnSe/CdSe nanocrystals with a core size of 4.0 nm and a shell thickness of 1−2 monolayers were prepared according to the literature method.[19,26] As expected, in the alloyed samples the Zn:Cd molar ratios measured in the XPS signals are in agreement with the elemental analysis results, while in the core−shell sample the molar ratio of shell to core element (Zn:Cd) from the XPS signals is significantly larger than the elemental analysis results (see Table 1).

Embryonic Nuclei-Induced Alloying Mechanism. Before the selection of the above-reported synthetic approach, we tried to prepare $Zn_xCd_{1-x}Se$-alloyed nanocrystals by the reaction of Zn and Cd precursors together with the injected Se precursor in the TOPO/HDA coordinating solvent system at high temperature. However, ZnSe and CdSe nucleated separately, which is indicated by the formation of two independent emission peaks in the PL spectrum corresponding to ZnSe and CdSe, respectively (refer to Supporting Information). In the identical coordinating solvent system, if Zn and Cd precursors were added sequentially, $Zn_xCd_{1-x}Se$ alloyed nanocrystals were formed via intermixing the Zn and Cd components together (Scheme 1), demonstrated by the sole emission peak in the spectrum.

It is known that the synthesis of nanocrystals in solution usually proceeds in two consecutive stages: nucleation and crystal growth.[28] In the process of nucleation, the newly formed nuclei are unstable until they reach a critical size (embryonic nuclei), where the nuclei solubility equals the monomer concentration. To reach the critical size, an energy barrier (i.e., nucleation barrier) needs to be overcome. Usually, the subsequent growth on the nuclei is more energetically favorable than the continuous formation of more nuclei because the nucleation process generally needs much higher activation energy than the particle growth.[28] If the embryonic nuclei are formed, a stable diffusion-driven growth process proceeds spontaneously. In essence, crystal growth has to be initiated with nuclei that are made by either imparting energy sufficient to overcome the nucleation energy or by adding foreign nuclei. When Zn and Cd precursors were introduced simultaneously, nucleation barrier energies needed to be overcome first. ZnSe and CdSe tend to nucleate separately due to the lattice mismatch between ZnSe and CdSe. The separate nucleation and epitaxial growth of CdSe and ZnSe by themselves should have their priority because the

SCHEME 1: Embryonic Nuclei-Induced Alloying Process for the Formation of Alloyed $Zn_xCd_{1-x}Se$ Nanocrystals

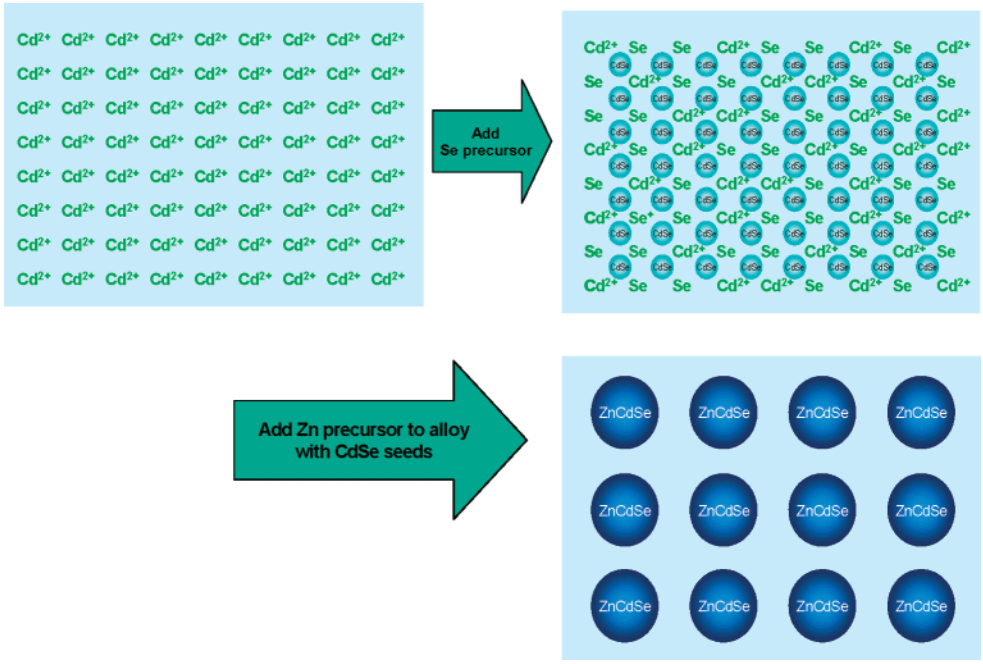

structural mismatch at the crystal interface between two different materials will give rise to the strain, which affects both the bulk free energy of nuclei and the interfacial free energy.

In our synthetic approach, a two-step synthetic procedure to alloyed nanocrystals was adopted to separate the nucleation process from the crystal growth. Embryonic CdSe nuclei (with size ~2 nm and emission wavelength ~480 nm, only the case of CdSe seeds was discussed) was prepared first through a rapid nucleation reaction. After the formation of CdSe nuclei, the Zn precursor was introduced into the reaction solution containing a large number of CdSe nuclei. No new ZnSe nuclei were formed because (i) the nucleation barrier energy needs to be overcome again before separate nucleation occurs and (ii) the continuous growth of the CdSe nuclei can decrease or lower the total free energy of the resulting nanocrystals. Moreover, the very stable Zn−TOPO complex is also helpful to avoid a new round of homogeneous nucleation in the synthetic system. As small CdSe seeds can induce "heterogeneous" growth on their surface through decreasing the total free energy of the system, the Zn complex in the solution may be transferred from solution and added continuously onto surfaces of individual CdSe seeds to grow them gradually into larger nanocrystals. Based on this microscopic nucleation mechanism, Zn/Se can alloy with the existing small CdSe nuclei seeds if the Zn precursor is directly added into the reaction system containing initially developed embryonic CdSe seeds in the presence of a large excess of Se precursor (Scheme 1) (or vice versa, by the incorporation of Cd/Se monomers into the initially formed embryonic ZnSe seeds). In other words, embryonic CdSe nuclei were prepared first as seeds, and the subsequent seeding growth of the CdSe nuclei can be separated from the nucleation process and thus allows the nuclei to grow into larger nanocrystals until the Zn and Cd precursors are depleted. These seeds may be capped with a ZnSe shell and can be transformed into uniform alloyed nanocrystals simultaneously through an atom interdiffusion process at high temperature as observed in the preparation of the previously reported $Zn_xCd_{1-x}E$ (E = Se or S) particles.[26,27] This is due to the increase of the diffusion coefficient and the depression of the melting point as the particle size decreases.[41,42] This approach is proven to be an effective way to produce high-quality short-wavelength-emitting $Zn_xCd_{1-x}Se$ nanocrystals with a narrow spectral width and high stability.

Conclusions

In summary, an embryonic nuclei-induced alloying approach has been developed for the formation of highly luminescent blue-emitting $Zn_xCd_{1-x}Se$ nanocrystals with narrow spectral width and high stability. A two-step synthetic procedure was designed to separate the CdSe (or ZnSe) nucleation process from the subsequent seeding growth of the $Zn_xCd_{1-x}Se$ nanocrystals. Small CdSe (or ZnSe) nuclei seeds can be made first, followed by the growth of these nuclei into $Zn_xCd_{1-x}Se$ nanocrystals, by incorporating the existing Cd/Se (or Zn/Se) monomers and the following injected Zn (or Cd) precursor together. A striking feature of the resulting alloyed nanocrystals is their unusual long-term stability of their emission wavelength/color, spectral width, and fluoresce efficiency at high temperature. The highly thermally stable $Zn_xCd_{1-x}Se$ nanocrystals can maintain a constant composition, identical size-distribution/particle size, and consistent brightness during a long period of heating (up to 7 h). The observed long-term stabilization of the emission wavelength and the particle size originated from the characteristic hardened structure of the alloy nanomaterials and the strong capping ligand system. Through this synthetic strategy, high-quality alloyed QDs with different desired emission wavelengths or colors can be made reproducibly by only changing details of the recipe through adding the predetermined amounts of reaction precursors. This nuclei-induced alloying process has been proven to be a practical method to make high-quality color-tunable nanocrystals. We expect that this alloying approach can be extended to synthesize other types of high-quality alloyed nanocrystal materials.

Acknowledgment. We gratefully acknowledge the Institute of Materials Research and Engineering, National University of Singapore, and Agency for Science, Technology, & Research for financial support.

Supporting Information Available: Synthetic procedure and PL spectra for separate nucleation. This material is available free of charge via the Internet at http://pubs.acs.org.

References and Notes

(1) For reviews, see Brus, L. E. *Appl. Phys. A* **1991**, *53*, 465. Banyai, L.; Koch, S. W. *Semiconductor Quantum Dots*; World Scientific: Singapore, 1993; Weller, H. *Angew. Chem., Int. Ed. Engl.* **1993**, *32*, 41. Weller, H. *Adv. Mater.* **1993**, *5*, 88; Alivisatos, A. P. *J. Phys. Chem.* **1996**, *100*, 13226; Heath, J. R. Ed. *Acc. Res.* **1999**, Special Issue for Nanostructures, review articles relevant to colloidal nanocrystals; *Handbook of Nanoctructured Materials and Nanotechnology*; Nalwa, H. S., Ed.; Academic Press: New York, 2000; Murray, C. B.; Kagan, C. R.; Bawendi, M. G. *Annu. Rev. Mater. Sci.* **2000**, *30*, 545.

(2) Colvin, V. L.; Schlamp, M. C.; Alivisatos, A. P. *Nature* **1994**, *370*, 354.

(3) Schlamp, M. C.; Peng, X.; Alivisatos, A. P. *J. Appl. Phys.* **1997**, *82*, 5837.

(4) Gao, M.; Lesser, C.; Kirstein, S.; Mohwald, H.; Rogach, A. L.; Weller, H. *J. Appl. Phys.* **2000**, *87*, 2297.

(5) Tessler, N.; Medvedev, V.; Kazes, M.; Kan, S. H.; Banin, U. *Science* **2002**, *295*, 1506.

(6) Klimov, V. I.; Mikhailovsky, A. A.; Xu, S.; Malko, A.; Hollingsworth, J. A.; Leatherdale, C. A.; Eisler, H. J.; Bawendi, M. G. *Science* **2000**, *290*, 314.

(7) Artemyev, M. V.; Woggon, U.; Wannemacher, R.; Jaschinski, H.; Langbein, W. *Nano Lett.* **2001**, *1*, 309.

(8) Bruchez, M. P.; Moronne, M.; Gin, P.; Weiss, S.; Alivisatos, A. P. *Science* **1998**, *281*, 2013.

(9) Chan, W. C. W.; Nie, S. *Science* **1998**, *281*, 2016.

(10) Han, M. Y.; Gao, X. H.; Su, J. Z.; Nie, S. M. *Nat. Biotechnology* **2001**, *19*, 631.

(11) Wu, X.; Liu, H.; Liu, J.; Haley, K. N.; Treadway, J. A.; Larson, J. P.; Ge, N.; Peale, F.; Bruchez, M. P. *Biotechnology* **2003**, *21*, 41.

(12) Jaiswal, J. K.; Mattoussi, H.; Mauro, J. M.; Simon, S. M. *Biotechnology* **2003**, *21*, 47.

(13) Murray, C. B.; Norris, D. J.; Bawendi, M. G. *J. Am. Chem. Soc.* **1993**, *115*, 8706.

(14) Talapin, D.; Rogach, A. L.; Kornowski, A.; Haase, M.; Weller, H. *Nano Lett.* **2001**, *1*, 207.

(15) (a) Qu, L.; Peng, X. *J. Am. Chem. Soc.* **2002**, *124*, 2049. (b) Peng, Z. A.; Peng, X. *J. Am. Chem. Soc.* **2001**, *123*, 183. (c) Qu, L.; Peng, Z. A.; Peng, X. *Nano Lett.* **2001**, *1*, 207.

(16) Hines, M. A.; Guyot-Sionnest, P. *J. Phys. Chem.* **1996**, *100*, 468.

(17) Peng, X.; Schlamp, M. C.; Kadavanich, A. V.; Alivisatos, A. P. *J. Am. Chem. Soc.* **1997**, *119*, 7019.

(18) Dabbousi, B. O.; Rodriguez-Viejo, J.; Mikulec, F. V.; Heine, J. R.; Mattoussi, H.; Ober, R.; Jensen, K. F.; Bawendi, M. G. *J. Phys. Chem. B* **1997**, *101*, 9463.

(19) Reiss, P.; Bleuse, J.; Pron, A. *Nano Lett.* **2002**, *2*, 781.

(20) Harrison, M. T.; Kershaw, S. V.; Burt, M. G.; Eychmuller, A.; Weller, H.; Rogach, A. L. *Mater. Sci. Eng., B* **2000**, *69*, 355.

(21) Korgel, B. A.; Monbouquette, H. G. *Langmuir* **2000**, *16*, 3588.

(22) Wang, W.; Germanenko, I.; El-Shall, M. S. *Chem. Mater.* **2002**, *14*, 3028.

(23) Kulkarni, S. K.; Winkler, U.; Deshmukh, N.; Borse, P. H.; Fink, R.; Umbach, E. *Appl. Surf. Sci.* **2001**, *169*, 438.

(24) Petrov, D. V.; Santos, B. S.; Pereira, G. A. L.; Donega, C. D. M. *J. Phys. Chem. B* **2002**, *106*, 325.

(25) Bailey, R. E.; Nie, S. *J. Am. Chem. Soc.* **2003**, *125*, 7100.

(26) Zhong, X.; Han, M.; Dong, Z.; White, T. J.; Knoll, W. *J. Am. Chem. Soc.* **2003**, *125*, 8589.

(27) Zhong, X.; Feng, Y.; Knoll, W.; Han, M. *J. Am. Chem. Soc.* **2003**, *125*, 13559.

(28) Sugimoto, T. *Monodisperse Particles*; Elsevier: 2001.

(29) Auer, S.; Frenkel, D. *Nature* **2001**, *409*, 1020.

(30) Demas, J. N.; Crosby, G. A. *J. Phys. Chem.* **1971**, *75*, 991.

(31) Vegard, L.; Schjelderup, H. *Phys. Z.* **1917**, *18*, 93.

(32) (a) Peng, X.; Wickham, J.; Alivisatos, A. P. *J. Am. Chem. Soc.* **1998**, *120*, 5343. (b) Peng, Z. A.; Peng, X. *J. Am. Chem. Soc.* **2001**, *123*, 1389. (c) Peng, X.; Manna, L.; Yang, W.; Wickham, J.; Scher, E.; Kadavanich, A.; Alivisatos, A. P. *Nature* **2000**, *404*, 59.

(33) Talapin, D. V.; Rogach, A. L.; Haase, M., Weller, H. *J. Phys, Chem. B* **2001**, *105*, 12278.

(34) Hines, M. A.; Guyot-Sionnest, P. *J. Phys. Chem. B*, **1998**, *102*, 3655.

(35) (a) Park, S.-J.; Kim, S.; Lee, S.; Khim, Z. G.; Char, K.; Hyeon, T. *J. Am. Chem. Soc.* **2000**, *122*, 8581. (b) Sun, S.; Muray, C. B.; Weller, D.; Folks, L.; Moser, A. *Science* **2000**, *287*, 1989.

(36) Shevchenko, E. V.; Talapin, D. V.; Rogach, A. L.; Kornowski, A.; Haase, M., Weller, H. *J. Am. Chem. Soc.* **2002**, *124*, 11480.

(37) Talapin, D. V.; Haubold, S.; Rogach, A.; L. Kornowski, A.; Haase, M. Weller, H. *J. Phys. Chem. B* **2001**, *105*, 2260.

(38) Shevchenko, E. V.; Talapin, D. V.; Schnablegger, H.; Kornowski, A.; Festin, O,; Svedlindh, P.; Haase, M., Weller, H. *J. Am. Chem. Soc.* **2003**, *125*, 9090.

(39) Donega, C. M.; Hickey, S. G.; Wuister, S. F.; Vanmaekelbergh, D.; Meijerink, A. *J. Phys. Chem. B* **2003**, *107*, 489.

(40) Kolomiets, B. T.; Ling, C. M. *Sov. Phys. Solid State* **1960**, *2*, 154.

(41) Shibata, T.; Bunker, B. A.; Zhang, Z.; Meisel, D.; Vardeman, C. F., II; Gezelter, J. D. *J. Am. Chem. Soc.* **2002**, *124*, 11996.

(42) Goldstein, A. N.; Echer, C. M.; Alivisatos, A. P. *Science* **1992**, *256*, 1425.